Science Press

ARTICLE

Effect of Calcination Atmospheres on Catalytic Performance of Pt/Al$_2$O$_3$ for Oxidation of CO and C$_3$H$_6$

Guo Miaoxin,   Wang Fengjun,   Wang Chengxiong,   Zhang Aimin,   Zhao Yunkun,   Du Junchen

State Key Laboratory of Advanced Technologies for Comprehensive Utilization of Platinum Metals, Kunming Institute of Precious Metals, Kunming 650106, China

Abstract: Pt/Al$_2$O$_3$ catalysts were prepared by an excess impregnation method with Pt(NH$_3$)$_2$(NO$_2$)$_2$ as the precursor. Then they were calcined in four different atmospheres (H$_2$, O$_2$, NO, NH$_3$), and characterized by N$_2$ adsorption and desorption test, X-ray diffraction, H$_2$-temperature programmed reduction (TPR) test, CO pulse adsorption test, and CO in-situ diffuse reflectance infrared Fourier transform spectroscopy (CO in situ DRIFTS). Results show that Pt/Al$_2$O$_3$ catalyst calcined in 1vol% H$_2$/N$_2$ atmosphere exhibits the best catalytic oxidation performance for CO and C$_3$H$_6$, because of the generation of numerous small-sized and highly dispersed Pt nanoparticles caused by the reducing calcination atmosphere.

Key words: Pt-based catalyst; calcination atmosphere; size effect; exhaust purification

Large amounts of CO and hydrocarbons (HC) are generated when the diesel engine is cold-started or the gas is insufficiently burned[1-4], which seriously endangers human health and living environment. The diesel oxidation catalyst (DOC) has been designed to oxidize these harmful pollutants into CO$_2$ and H$_2$O[5-7]. In addition, the sulfur compounds contained in diesel fuel poison and inactivate the catalyst during operation[8,9]. Therefore, since the advent of catalytic converters for diesel locomotives, platinum has been widely used due to its strong sulfur resistance and high activity against CO and HC oxidation[1,3,5,10]. Pt-based DOC is usually used in metal oxides. Alumina with large surface areas, good adsorption performance, moderate chemical activity, and low cost is a common support for DOC[1,8,10,11]. Their combination makes Pt/Al$_2$O$_3$ a good model catalyst for DOC and has been reported by numerous articles.

DOC normally requires a highly dispersed Pt state, because with increasing the reaction surface area of Pt particles, the activity generally increases and the cost decreases[7]. Previous researches have explored many factors affecting the dispersion or particle size of Pt/Al$_2$O$_3$, such as preparation method (processing conditions, atmosphere, time, temperature)[8,12-14], precious metal precursor[13,15,16], and modified additives[17-21]. The catalyst structure and performance mainly depend on the preparation method[8,22]. However, the effect of calcination atmospheres on catalyst characteristics is barely investigated.

Guo et al[14] treated the Pt/Al$_2$O$_3$ catalyst in an atmosphere containing H$_2$, He, N$_2$, O$_2$, and various chlorine compounds, and confirmed that the treatment atmosphere has a significant effect on the Pt crystallite size and size distribution through H$_2$ chemisorption test and wide-angle X-ray diffraction (XRD) analysis. However, the research is not applied to any actual reaction. Huang et al[23] used base metal Cu instead of precious Pt and studied the effect of calcination atmospheres on Cu/γ-Al$_2$O$_3$ catalyst for CO oxidation. It is found that the oxidizing calcination atmosphere (air) leads to a re-dispersed copper surface but a dramatically reduced activity, whereas the calcination in the reducing atmosphere (10vol% H$_2$/N$_2$) produces a strong metal-support interaction which causes the substantial increase in activity. Hansen et al[8] calcined the Pt/Al$_2$O$_3$ catalysts in N$_2$ and/or O$_2$ atmosphere and found that the catalyst with Pt particles of 2~4 nm in diameter has the

optimal performance for CO and HC oxidation. Hu et al[13] found that using flowing gas instead of static air during calcination leads to higher Pt dispersion.

In automobile exhaust, the gaseous atmosphere is either oxidizing or reducing atmosphere. In this research, the Pt/Al_2O_3 catalysts with Pt nanoparticles of 2~4 nm in diameter were prepared and the effects of four different flowing oxidizing or reducing calcination atmospheres on the oxidation reactions of CO and C_3H_6 related to DOC were investigated.

1 Experiment

Pt/Al_2O_3 catalysts with a constant Pt loading amount of 1.5wt% (theoretical value) were synthesized by an excess impregnation method with $Pt(NH_3)_2(NO_2)_2$ as metal precursor. After the catalysts were dried overnight at 393 K, they were cut into blocks, calcined in different atmospheres of 1vol% H_2, 1vol% O_2, 0.1vol% NH_3, and 0.1vol% NO (balanced with N_2) in the muffle furnace at 823 K for 2 h, and labeled as Pt/Al (1% H_2), Pt/Al(1% O_2), Pt/Al(0.1% NH_3) and Pt/Al(0.1% NO), respectively.

The specific surface area and pore size distribution of powder specimens were determined through nitrogen adsorption and desorption test at 77 K by the Quantachrome NOVA2000e physisorption apparatus. The specific surface area was calculated by the Brunauer-Emmett-Teller (BET) method, and pore volume and pore size distributions were determined by Barrett-Joyner-Halenda (BJH) model.

The phase composition was recorded by the Rigaku D/MAX-2000 automatic XRD with Cu Kα radiation ($\lambda = 0.15406$ nm), scanning range of 10°~90°, and step size of 0.02°.

Hydrogen temperature programmed reduction (H_2-TPR) experiments were carried out on a Quantachrome CHEMBET 3000 chemisorption instrument. The specimen of 100 mg was placed in a quartz U-tube reactor and pretreated in Ar at 373 K for 30 min before testing. After cooling to room temperature, the mixed H_2/Ar gas with a flow rate of 75 mL·min^{-1} was introduced, and then the temperature was raised to 1073 K with a rate of 10 K·min^{-1}.

In situ diffuse reflectance infrared Fourier transform spectroscopy (DRIFTS) test was conducted by a Themo Nicolet 6700 FT-IR spectrometer equipped with mercury cadmium telluride (MCT) detector. In-situ reaction cell with ZnSe window allowed specimen of 15 mg to be heated to 773 K under specific atmospheric pressure. Before each test, the pipeline was purged by N_2 for 30 min and then cooled to the desired temperature. The background was collected before switching N_2 with the reaction gas (pure CO). When the catalyst was at the saturated adsorption state, the residual and physically adsorbed CO gas in the pipeline was purged by the N_2 flow, and the spectrum was recorded (average of 32 scans at 4 cm^{-1} resolution) at each schedule time.

The Quantachrome CHEMBET 3000 chemisorption instrument was employed in CO pulse adsorption procedure. Assuming that all CO was adsorbed by Pt atoms, the dispersion of Pt was calculated by the stoichiometric factor of

1 CO/Pt. Each specimen was pre-reduced with H_2/He at 723 K for 2 h with a flow rate of 75 mL·min^{-1}. The reaction furnace temperature dropped to 353 K and stabilized for 30 min. Then the high-purity CO was inflated by pulsed injection until the signal detected by the thermal conductivity detector (TCD) no longer changed.

The catalytic activity for CO and C_3H_6 was evaluated in a quartz tube fixed bed continuous flow reactor (8 mm in inner diameter and 50 mm in length). The catalysts with a particle size of 380~250 μm were sieved after tableting and selected as the test medium. The reaction atmosphere consisted of 1vol% CO or 0.3vol% C_3H_6+5vol% O_2+balance gas N_2 with gas hourly space velocity (GHSV) of 18 000 mL·h^{-1}·g^{-1}. A pre-calibrated mass flow meter was used to control the gas flow in each gas path, and a thermocouple was inserted on the fixed reaction bed to monitor the real-time reaction temperature. The exhaust gas dried by magnesium chloride entered the Agilent 7890A gas chromatograph equipped with two TCDs and a hydrogen flame ionization detector (FID) for online analysis. The detector operating temperature was 393 K, and H_2 was the carrier gas.

The catalytic conversion of CO and C_3H_6 was calculated by Eq.(1) as follows:

$$X = \frac{C_{in} - C_{out}}{C_{in}} \times 100\% \tag{1}$$

where C_{in} and C_{out} represent the inlet and outlet concentrations of CO or C_3H_6, respectively.

2 Results and Discussion

2.1 N_2 adsorption-desorption test

The textural properties of Pt/Al_2O_3 catalysts calcined in different atmospheres are listed in Table 1. The specific surface of Pt/Al_2O_3 catalysts is larger than that of pure Al_2O_3 support, indicating that the acidic $Pt(NH_3)_2(NO_2)_2$ solution corrodes the pore structure on the support surface and slightly increases the reaction area. All N_2 adsorption-desorption isotherms of four specimens have obvious hysteresis loops (Fig.1a), which is ascribed to the mesoporous material[24].

The pore size distributions are also basically the same (Fig.1b), showing that the physical properties of the prepared specimens have no significant variance despite the different calcination atmospheres.

2.2 XRD analysis

Fig. 2 shows the XRD patterns of different Pt/Al_2O_3 catalysts. Characteristic diffraction peaks of γ -Al_2O_3 (JCPDS No. 46-1131) can be clearly identified, revealing the high dispersion of platinum particles on the Al_2O_3 surface regardless of the oxidizing atmosphere (O_2 or NO) or the reducing atmosphere (H_2 or NH_3). Moreover, the peak position and peak intensity of XRD patterns of all specimens are highly similar, demonstrating that the calcination atmosphere does not affect the crystal structure of catalysts.

2.3 Pt particle size

Qualitative and semi-quantitative analyses of Pt particle size in the Pt/Al_2O_3 catalyst were performed using the CO in

Table 1   Textural parameters of support Al_2O_3 and different Pt/Al_2O_3 catalysts

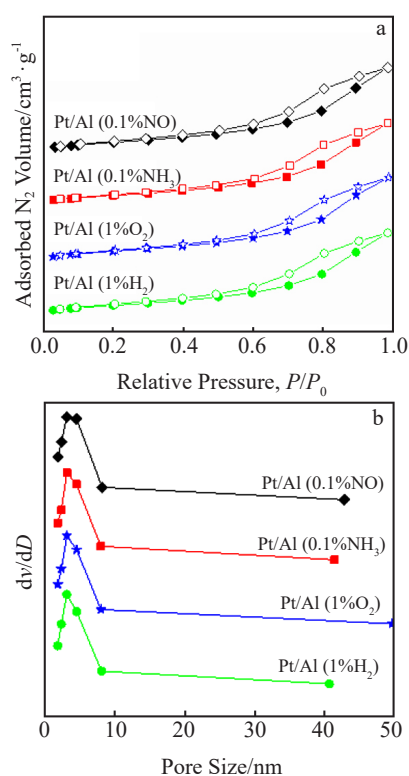| Specimen	Specific surface area/$m^2 \cdot g^{-1}$	Pore size/nm	Pore volume/$cm^3 \cdot g^{-1}$	Pt dispersion/%	Pt particle size/nm
Al_2O_3	158.5	3.2	0.4195	-	-
$Pt/Al(1\%H_2)$	166.4	3.1	0.4279	24.61	2.3
$Pt/Al(1\%O_2)$	169.5	3.1	0.4293	20.21	2.8
$Pt/Al(0.1\%NH_3)$	168.7	3.1	0.4278	16.65	3.4
$Pt/Al(0.1\%NO)$	168.9	3.0	0.4268	16.17	3.5

Note: Pt particle size is estimated through dispersion data.

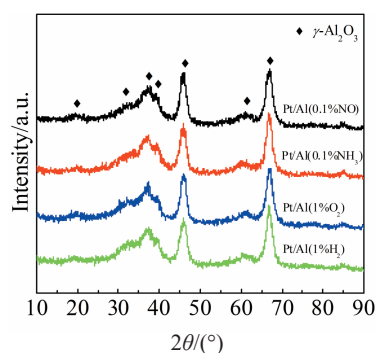Fig.1 N_2 adsorption-desorption isotherms (a) and pore size distributions (b) of different Pt/Al_2O_3 catalysts

Fig.2   XRD patterns of different Pt/Al_2O_3 catalysts

situ DRIFTS characterization technique. The results are shown in Fig. 3 and Table 1. The peaks near 1825 cm^{-1} are related to the bridge adsorption of CO by Pt atoms, while the peaks close to 2050 cm^{-1} refer to the linear adsorption of CO by Pt atoms in the Pt/Al_2O_3 catalyst[25]. Based on previous researches[26], Pt nanoparticle size is positively related to the number of Pt-Pt bonds, which leads to the fact that small Pt particles provide large charge density to the $2\pi^*$ orbital of the adsorbed CO. Hence, different intensities between linear adsorption and bridge adsorption in the spectra are associated with the Pt particle size in different catalysts. The stronger the linear adsorption, the weaker the bridge adsorption and the smaller the Pt particle size in the catalyst[8]. As shown in Fig.3, $Pt/Al(1\%H_2)$ catalyst has the highest intensity ratio of linear adsorption to bridged adsorption, indicating that its Pt particles are the smallest. However, the conclusion should be exactly the opposite for $Pt/Al(0.1\%NH_3)$ and $Pt/Al(0.1\%NO)$.

The results of CO pulse adsorption experiment are presented in Table 1, revealing that different calcination atmospheres cause changes of Pt particle size in Pt/Al_2O_3 with the order of $Pt/Al(1\%H_2)$ <$Pt/Al(1\%O_2)$ <$Pt/Al(0.1\%NH_3)$ < $Pt/Al(0.1\%NO)$. This may be due to the decomposition of $Pt(NH_3)_2(NO)_2$ precursor. When the catalysts are calcined in an atmosphere containing decomposition products (NH_3 or NO), according to Le Châtelier's principle, the decomposition rate of $Pt(NH_3)_2(NO)_2$ slows down, resulting in the poor dispersion of Pt particles. When the catalysts are calcined under 1vol% H_2/N_2 atmosphere, H_2 not only reacts with NO to accelerate the decomposition of $Pt(NH_3)_2(NO)_2$ precursor, but also further reduces the PtO_x generated by the decomposition to Pt, achieving the effect of re-dispersion.

2.4 H_2-TPR test

H_2-TPR experiment was performed to investigate the effect of calcination atmospheres on the reduction performance of
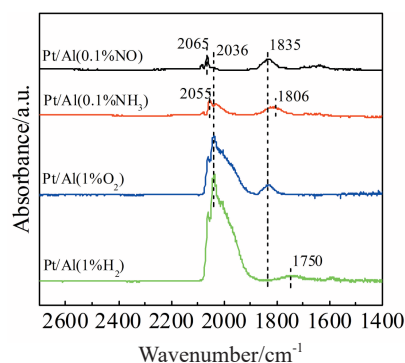

Fig.3   CO in situ DRIFTS spectra of different Pt/Al_2O_3 catalysts

Pt/Al_2O_3 catalysts. As shown in Fig. 4, each catalyst has two distinct reduction peaks. The low-temperature hydrogen reduction peak (381~408 K) can be attributed to the reduction of highly dispersed ultrafine Pt nanoparticles, while the high-temperature hydrogen reduction peak is related to the reduction of large Pt particles[4,27,28].

The catalysts are inevitably oxidized by the air during storage and use at room temperature; the longer the exposure time in air, and the higher the dispersion, the higher the degree of oxidation, i.e., highly dispersed Pt particles are easily to be oxidized[29,30]. In addition, for transition metal oxides, the reduction temperature is mainly affected by the particle size. The smaller the oxide particle size, the higher the concentration of the oxygen vacancies and sites responsible for activate H_2[15,31,32]. Among the four catalysts, the Pt/Al_2O_3 (1%H_2) catalyst has the highest dispersion and the smallest Pt particle size, which is more likely to be oxidized at room temperature, resulting in the lowest reduction temperature and highest H_2 consumption in the corresponding TPR profiles, and the results of Pt/Al(0.1%NO) catalyst are just the opposite.

Due to the difference in composition and component content, although NH_3 and H_2 both belong to the reducing calcination atmosphere, the reduction performance of the Pt/Al_2O_3 specimen calcined in the former atmosphere is still far lower than the latter.

2.5 Catalytic activity

Fig. 5 and Table 2 show that different calcination atmospheres lead to very different performances of Pt/Al_2O_3 for CO and C_3H_6 oxidation. Among these catalysts, the catalyst calcined in 1vol% H_2/N_2 atmosphere exhibits the best catalytic performance. As shown in Table 2 and Fig.5, the Pt/Al(1%H_2) has the highest conversion efficiency and the lowest conversion temperature for CO and C_3H_6 oxidation. The reduction ability improves (confirmed by H_2-TPR test) and the formation of numerous fine Pt particles in the CO pulse adsorption experiment explains the improvement mechanism. The ultrafine platinum particles can effectively enhance the catalytic oxidation activity due to the cluster size effect or structural sensitivity[27,33-35]. With the same Pt content, the smaller Pt cluster has a larger surface area to volume ratio, which can provide more potential active sites for surface Pt
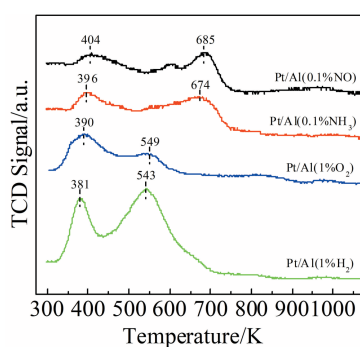
atoms to participate in the reaction; thus better catalytic properties are achieved[36-38]. In addition, the enhancement mechanism may be due to hydroxyl groups (-OH). It is reported that the -OH group formed by H_2 and O_2 can promote the CO oxidation on Pt(111)[39-41].

For the Pt/Al(1%O_2) catalyst, due to the large excess of oxygen presented during the calcination stage, smaller Pt particles are easily oxidized to PtO_x, resulting in the loss of active components in platinum metal, which has a negative influence on the catalytic performance[1,27,42-45]. Therefore, Pt/Al (1%O_2) catalyst shows moderate CO oxidation performance (T_{50}=420 K, T_{90}=430 K).

Catalysts with excellent reduction properties are beneficial to effective purification of CO and hydrocarbons in exhaust gases[27]. Pt/Al(0.1%NH_3) and Pt/Al(0.1%NO) catalysts are basically equivalent and unsatisfactory for CO convention because of their large particle size and poor reduction ability for PtO_x.

Furthermore, the four catalysts show the similar regularity in the C_3H_6 oxidation experiment. However, because the length of the C=C bond is shorter and the bond energy is
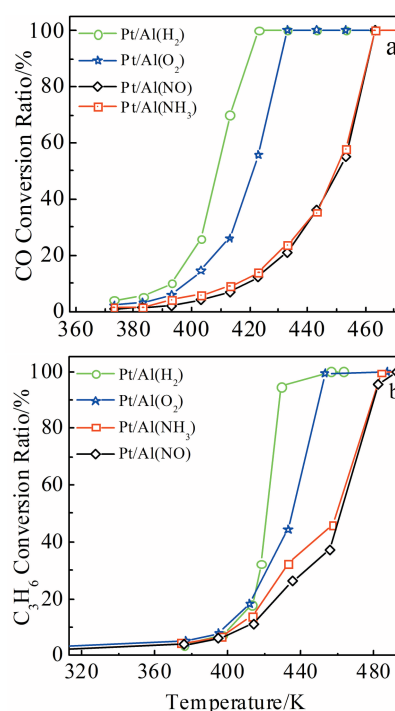
Fig.5 CO (a) and C_3H_6 (b) oxidation results of different Pt/Al_2O_3 catalysts

Fig.4 H_2-TPR results of different Pt/Al_2O_3 catalysts

Table 2 T_{50} and T_{90} of different Pt/Al_2O_3 catalysts (K)

Specimen	T_{50}		T_{90}	
	CO	C_3H_6	CO	C_3H_6
Pt/Al(1%H_2)	408	420	419	428
Pt/Al(1%O_2)	420	434	430	449
Pt/Al(0.1%NH_3)	449	458	460	478
Pt/Al(0.1%NO)	449	460	460	478

larger than that of C=O bond, the Pt/Al_2O_3 catalyst more easily achieves the complete CO oxidation than C_3H_6 oxidation.

3 Conclusions

1) Different oxidizing or reducing atmospheres do not affect the pore structure or crystal structure of Pt/Al_2O_3 catalysts, but cause differences in the particle size and dispersion of precious metals.

2) The catalyst calcined under 1vol% H_2/N_2 atmosphere exhibits the highest conversion efficiency and the lowest conversion temperature for CO and C_3H_6 oxidation. This research provides a simple and economical method to improve the catalytic performance of diesel oxidation catalysts.

References

1   Russell A, Epling W S. *Catalysis Reviews: Science and Engineering*[J], 2011, 53(4): 337

2   Katare S R, Patterson J E, Laing P M. *Industrial & Engineering Chemistry Research*[J], 2007, 46(8): 2445

3   Twigg M V. *Catalysis Today*[J]. 2006, 117(4): 407

4   Yang Chaoqin, Wang Yaming, Wu Legang. *Rare Metal Materials and Engineering*[J], 2017, 46(8): 2049

5   Dadi R K, Luss D, Balakotaiah V. *Chemical Engineering Journal* [J], 2016, 304(6): 941

6   Raj R, Harold M P, Balakotaiah V. *Chemical Engineering Journal*[J], 2015, 281(6): 322

7   Haaß F, Fuess H. *Advanced Engineering Materials*[J], 2005, 7(10): 899

8   Hansen T K, Høj M, Hansen B B *et al*. *Topics in Catalysis*[J], 2017, 60(17-18): 1333

9   Corro G. *Reaction Kinetics and Catalysis Letters*[J], 2002, 75(1): 89

10 Hirata H. *Catalysis Surveys from Asia*[J], 2014, 18(4): 128

11 Du Junchen, Ma Jiangli, Wang Fengjun *et al*. *Chinese Journal of Inorganic Chemistry*[J], 2018, 34(4): 800

12 Abedi A, Luo J Y, Epling W S. *Catalysis Today*[J], 2013, 207(5): 220

13 Hu L J, Boateng K A, Hill J M. *Journal of Molecular Catalysis A: Chemical*[J], 2006, 259(1-2): 51

14 Guo I, Yu T T, Wanke S E. *Studies in Surface Science and Catalysis*[J], 1988, 38(2): 21

15 Borges L R, Lopez-Castillo A, Meira D M *et al*. *ChemCatChem* [J], 2019, 11(13): 3064

16 Svintsitskiy D A, Kibis L S, Stadnichenko A I *et al*. *ChemCatChem*[J], 2020, 12(3): 867

17 Zhong F L, Zhong Y J, Xiao Y H *et al*. *Catalysis Letters*[J], 2011, 141(12): 1828

18 Wang H, Dong J S, Allardc L F *et al*. *Applied Catalysis B: Environmental*[J], 2019, 244(11): 327

19 Kolli T, Kanerva T, Huuhtanen M *et al*. *Catalysis Today*[J], 2010, 154(3-4): 303

20 Wan J, Ran R, Li M *et al*. *Journal of Molecular Catalysis A: Chemical*[J], 2014, 383-384(9): 194

21 Lee C H, Chen Y W. *Industrial & Engineering Chemistry Research*[J], 1997, 36(5): 1498

22 Monyanon S, Luengnaruemitchai A, Pongstabodee S. *International Journal of Hydrogen Energy*[J], 2010, 35(8): 3234

23 Huang T J, Yu T C, Chang S H. *Applied Catalysis*[J], 1989, 52(1): 157

24 Sing K S W, Everett D H, Haul R A W *et al*. *Pure & Applied Chemistry*[J], 1985, 57(4): 603

25 Bourane A, Dulaurent O, Bianchi D. *Langmuir*[J], 2015, 17(8): 5496

26 Fanson P T, Delgass W N, Lauterbach J. *Journal of Catalysis*[J], 2001, 204(1): 35

27 Yang Z Z, Li J, Zhang H L *et al*. *Catalysis Science & Technology* [J], 2015, 5(4): 2358

28 Haneda M, Watanabe T, Kamiuchi N *et al*. *Applied Catalysis B: Environmental*[J], 2013, 142-143(4): 8

29 Lee A F, Gee J J, Theyers H J. *Green Chemistry*[J], 2000, 2(6): 279

30 Lee A F, Wilson K, Lambert R M *et al*. *Journal of Catalysis*[J], 1999, 184(2): 491

31 Hwang C P, Yeh C T. *Journal of Molecular Catalysis A: Chemical*[J], 1996, 112(2): 295

32 Rodriguez A, Hanson J C, Frenkel A I *et al*. *Journal of the American Chemical Society*[J], 2002, 124(2): 346

33 Nethravathi C, Anumol E A, Rajamathib M *et al*. *Nanoscale*[J], 2011, 3(2): 569

34 Lu J L, Stair P C. *Angewandte Chemie International Edition*[J], 2010, 122(14): 2601

35 Murzin D Y. *Catalysis Science & Technology*[J], 2014, 4(9): 3340

36 Lei Y, Zhao H Y, Rivas R D *et al*. *Journal of the American Chemical Society*[J], 2014, 136(26): 9320

37 Bonanni S, Aït-Mansour K, Harbich W *et al*. *Journal of the American Chemical Society*[J], 2014, 136(24): 8702

38 Wei J M, Iglesia E. *Journal of Physical Chemistry B*[J], 2004, 108(13): 4094

39 Minemura Y, Ito S I, Miyao T *et al*. *Chemical Communications* [J], 2005, 25(11): 1429

40 Yakovkin I N, Chernyi V I, Naumovets A G. *Surface Science*[J], 1999, 442(1): 81

41 Bergeld J, Kasemo B, Chakarov D V. *Surface Science*[J], 2001, 495(3): 815

42 Kreuzer T, Lox E S, Lindner D *et al*. *Catalysis Today*[J], 1996, 29(1): 17

43 Yang Z Z, Chen Y D, Zhao M *et al*. *Chinese Journal of Catalysis* [J], 2012, 33(5): 819

44 Hauff K, Tuttlies U, Eigenberger G *et al*. *Applied Catalysis B: Environmental*[J], 2012, 123-124(2): 107

45 Smeltz A D, Delgass W N, Ribeiro F H. *Langmuir*[J], 2010, 26(21): 16 578

焙烧气氛对Pt/Al$_2$O$_3$催化氧化CO和C$_3$H$_6$性能的影响

郭淼鑫，王凤军，王成雄，张爱敏，赵云昆，杜君臣

(昆明贵金属研究所 稀贵金属综合利用新技术国家重点实验室，云南 昆明 650106)

摘　要： 使用Pt(NH$_3$)$_2$(NO$_2$)$_2$作为前驱体，通过过量浸渍法制备Pt/Al$_2$O$_3$催化剂，并将其在4种不同的气氛（H$_2$、O$_2$、NO或NH$_3$）中进行焙烧。利用N$_2$吸脱附、X射线衍射、程序升温还原（H$_2$-TPR）、CO脉冲吸附、CO原位漫反射傅里叶变换红外光谱（CO in situ DRIFTS）等手段对催化剂的物化性质进行了表征。结果表明：由于还原性焙烧气氛导致了众多小尺寸和高分散的Pt纳米颗粒的生成，经1%（体积分数）H$_2$/N$_2$焙烧的Pt/Al$_2$O$_3$表现出最佳的CO和C$_3$H$_6$催化氧化性能。

关键词： Pt基催化剂；焙烧气氛；尺寸效应；尾气净化

作者简介：郭淼鑫，男，1997年生，硕士生，昆明贵金属研究所稀贵金属综合利用新技术国家重点实验室，云南 昆明 650106，电话：0871-68316562，E-mail：miaoxin_guo@163.com